Ultrafast charge-transfer processes at an oriented phthalocyanine/C_{60} interface

G. J. Dutton,[1] W. Jin,[2] J. E. Reutt-Robey,[2] and S. W. Robey[1]
[1]*National Institute of Standards and Technology, 100 Bureau Drive, Gaithersburg, Maryland 20899, USA*
[2]*Department of Chemistry and Biochemistry, University of Maryland, College Park, Maryland 20742, USA*
(Received 9 July 2010; published 19 August 2010)

The ultrafast dynamics at a well-characterized CuPc/C_{60} organic photovoltaic heterojunction have been directly measured with time-resolved two-photon photoemission (TR-2PPE). Phthalocyanine/C_{60} donor-acceptor interfaces, characterized in detail via scanning tunneling microscopy, provide model systems for studies of critical charge separation and recombination processes that determine device performance. TR-2PPE studies of copper phthalocyanine (CuPc)/C_{60} interfaces reveal ultrafast charge separation and provide evidence for recombination via low-lying CuPc triplet levels.

DOI: 10.1103/PhysRevB.82.073407 PACS number(s): 73.50.Pz, 78.40.Me, 78.47.J−, 88.40.jr

Photocurrent production in organic photovoltaic structures differs markedly from inorganic solar cells. Dissociation of excitons to produce free carriers in organic devices requires interfaces between a donor and acceptor to provide the driving force for charge separation.[1] Recent theoretical work has highlighted the impact of interfacial molecular structure on the competition between charge pair dissociation and recombination.[2] Improvements in device efficiency can be hastened by unraveling the dynamics of charge transfer and recombination and establishing correlations with interfacial molecular and electronic structure.

Ultrafast optical and terahertz studies of polymer blend and multilayer photovoltaic systems have probed charge separation processes into the subpicosecond regime,[3–5] producing much useful insight. For instance, recent work has highlighted the potential impact of bound interfacial charge-transfer (ICT) states on charge separation.[6,7] However, it is difficult to correlate information from these techniques directly with characteristics of the interfaces. Time-resolved two-photon photoemission (TR-2PPE) provides the necessary sensitivity to the donor-acceptor interfacial region.[8] Previous studies have demonstrated the utility of TR-2PPE to investigate image state dynamics at organic surfaces[9] and electron transfer at molecule-inorganic semiconductor interfaces.[10,11] When coupled with molecular structure information from scanning tunneling microscopy, this allows correlation of interfacial molecular and electronic structure with the dynamics of charge separation.

In this Brief Report, we provide results from TR-2PPE studies of exciton dynamics at a well-characterized organic donor-acceptor interface. The donor-acceptor system chosen for this work, copper phthalocyanine (CuPc) and C_{60}, has been studied extensively for small molecule solar cells, producing promising efficiencies.[12] When CuPc or ZnPc are deposited on well-ordered, hexagonal C_{60} surfaces, scanning tunneling microscopy (STM) (Refs. 13 and 14) reveals ordered phthalocyanine step heights >1 nm, indicating that the molecules adopt an "upright" orientation, with the molecular plane nearly perpendicular to the interface with the underlying C_{60} molecules, as illustrated schematically at the bottom of Fig. 1. This provides an oriented model organic photovoltaic interface for study of the dominant relaxation processes using TR-2PPE.

Photoemission, both one and two photon, was performed in an ultrahigh-vacuum system equipped for organic deposition. The Ag(111) substrate was cleaned by sputtering and annealing, and films were deposited at typical rates of ~0.05 monolayer (ML) equivalents min^{-1}, with coverage based on measured work function change and image state analysis. A C_{60} monolayer was deposited at 300 °C with additional epitaxial layers up to 20 ML deposited at 150 °C to provide a bulklike fullerene substrate. CuPc was subsequently deposited to thicknesses from 1 to 5 ML at a substrate temperature of 40 °C.

TR-2PPE and ultraviolet photoelectron spectroscopy (UPS) data were collected with a hemispherical analyzer. The laser source was a tunable Ti:sapphire oscillator (150 fs pulse width). The pump was focused to a 100-μm-diameter spot, producing a peak power density of 0.3 GW/cm^2, while the probe had a significantly lower power density. The beams were noncollinearly overlapped at the sample with perpendicular polarizations (s pump, p probe) to eliminate coherent two-color photoemission. Polarization-dependent photoemission data (not shown) were consistent with the upright CuPc orientation observed in STM.

The alignment of donor and acceptor electronic bands is critical to photovoltaic performance. The band diagram for this specific interface, included in Fig. 1, is based on UPS and 2PPE results from this work, with errors of ±0.1 eV, complemented with previous inverse photoemission spectroscopy (IPES).[15] UPS for 20 ML C_{60}/Ag(111) places the C_{60} highest-occupied molecular orbital (HOMO) at −2.1 eV with respect to E_F. The HOMO of CuPc (5 ML) on 20 ML C_{60} is located at −1.09 eV, in good agreement with a previous report for this interface.[16] The location of ICT and CuPc triplet levels will be discussed below. Optical absorption in CuPc is represented in the figure with the photohole in the HOMO to emphasize the energy offset that impacts electron transfer to C_{60}.

The lowest optical absorption in bulk metal phthalocyanines, the Q band, arises from $\pi \rightarrow \pi^*$ transitions from the a_{1u} HOMO to the e_{1g} lowest unoccupied molecular orbital (LUMO), producing a band centered at ~650 nm and extending to 800 nm.[17] The dipole moment is oriented in the molecular plane. The excitation scheme for TR-2PPE employed the Ti:sapphire fundamental at 750 nm (1.65 eV) as pump and the 4.96 eV third harmonic as probe. This is a compromise designed to produce sufficient absorption in CuPc by the pump while reducing the one-photon background from the UV probe. Absorption in C_{60} at 1.65 eV is

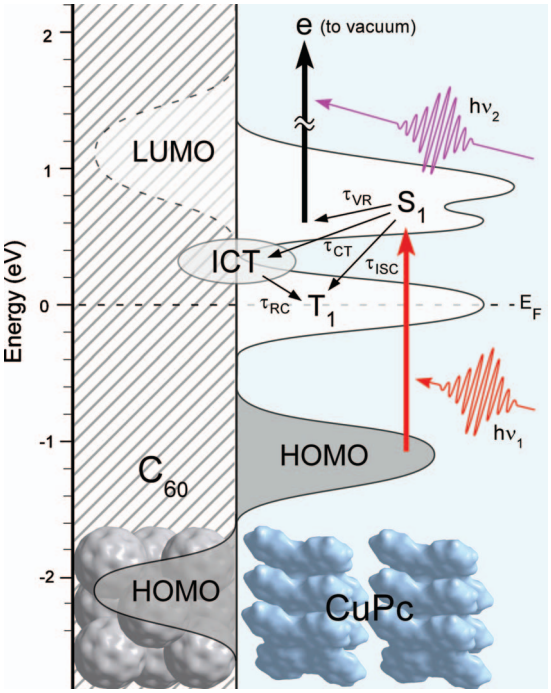

FIG. 1. (Color) Energy-level diagram for CuPc/C_{60}/Ag(111) as probed by photoelectron, inverse photoelectron, and optical spectroscopies; all energies with respect to E_F. (S_1,T_1=singlet, triplet excitons; ICT=interfacial charge transfer state). The excitation scheme is indicated along with dominant decay channels. For a discussion, see the text.

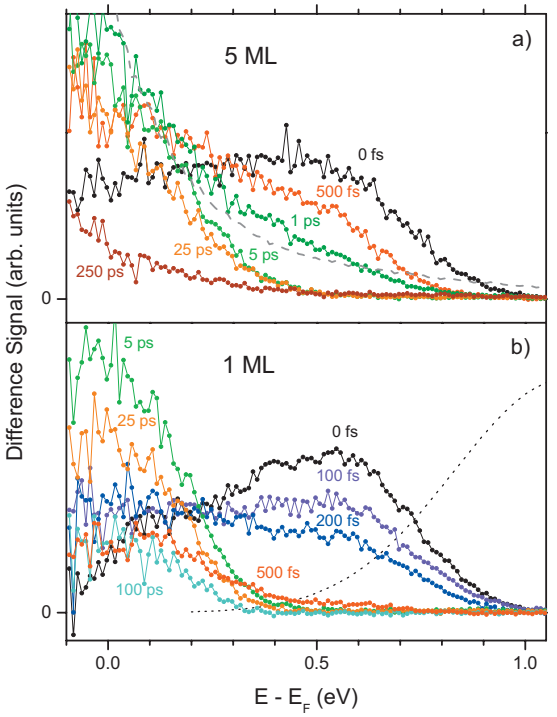

FIG. 2. (Color) Pump-probe difference spectra at fixed delays for (a) 5 ML and (b) 1 ML CuPc on 20 ML C_{60}, as a function of intermediate state energy above the Fermi level. A typical background (dashed line) is shown in (a). A simulated IPES spectrum (dotted line) for bulk C_{60} is included in (b).

negligible;[18] thus, the initial excitation product is predominantly the lowest energy CuPc singlet (S_1) exciton. 2PPE investigations of C_{60} and CuPc multilayers confirmed that pumping at 1.65 eV yielded no measurable response for pure C_{60} films, whereas transitions to phthalocyanine excitonic levels were observed in thick CuPc films. For these CuPc/C_{60} structures, 2PPE measurements are dominated by signal from the outermost CuPc layer due to photoelectron attenuation[19] in the upright oriented CuPc layers.

The impact of pumping the CuPc molecular layers is evident in the difference spectra (pump+probe minus probe only) displayed in Fig. 2. A rising probe-only background [dashed line, Fig. 2(a)] at low energy is due to one-photon photoemission by the UV probe, which exceeds the work function of 4.30 eV. Simultaneous illumination with the pump produces an increase above this one-photon edge arising from pump-induced CuPc S_1 excitonic intermediate states approximately $-1.09+1.65=0.56$ eV above E_F that are subsequently ionized by the UV probe.

Dynamics of these excitations were investigated by introducing variable pump-probe delays, from −1 (probe before pump) to 250 ps. Fixed-delay spectra for junctions of 5 and 1 ML CuPc on C_{60} are shown in Fig. 2. Focusing first on the 5 ML data [Fig. 2(a)], we see that excitations above ~0.4 eV decay monotonically and are depleted by 5 ps. A shift of spectral weight to lower energies accompanies this loss in intensity above 0.4 eV. During this same time period, the population below 0.4 eV increases, reaching a maximum after several picoseconds, followed by a slow decay of hundreds of picoseconds. The total spectral density integrated over all energies (not shown) decreases by <30% in the first several picoseconds, suggesting that the decrease in population above 0.4 eV is predominantly transferred to the lower energy regions.

Turning to 1 ML CuPc [Fig. 2(b)], we note that the pump-induced structure at $t=0$ is similar to the thick film, with slight differences in detailed shape. Intensity above ~0.4 eV again decays rapidly with a rate that is much faster than for the 5 ML structure. The S_1 population above 0.4 eV is completely depleted by 500 fs. Also contrary to 5 ML, the intensity in this region shows no appreciable spectral downshift. Qualitative differences are also evident in the low-energy region of the spectrum. In the time up to 500 fs, while the population above 0.4 eV undergoes very rapid decay, intensity below that point does not increase for the 1 ML sample—note the 500 fs spectrum. The total intensity over the whole spectral region (not shown) is reduced by a factor of at least 3 in the first 500 fs. An increase at low energy occurs only well after decay at high energy is complete, again reaching a maximum by ~5 ps. Thus, at the interface, depletion of the original singlet population is complete before intensity begins to appear at low energy. After this delayed rise, however, the subsequent slow decay at low energy is similar in both samples.

For greater dynamical detail, cross-correlation measurements were performed to provide time-dependent information at fixed energies. The curves in Fig. 3 are normalized to the maximum value to emphasize *differences* in decay behavior. Fits employing a sum of exponentially decaying step functions convolved with the instrumental response are in-

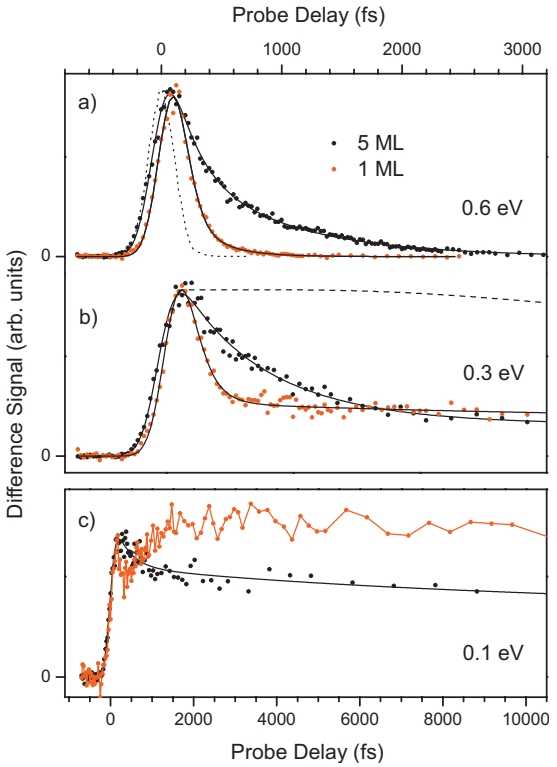

FIG. 3. (Color) Cross-correlation traces at selected energies. Smooth solid lines are fits to the data. The dotted line in (a) is the instrumental response [from the Ag(111) surface state] and the dashed line in (b) is the result of exciton diffusion simulation. Note the difference in time-axis scaling between (a), (b) and (c).

cluded as solid lines. These fits will not rigorously model the decay dynamics but do provide a quantitative assessment of the characteristic time scales.

Cross-correlation curves acquired at high energy [Fig. 3(a)] clearly reflect the ultrafast decay in the 1 ML structure. The 1 ML cross correlation is nearly symmetric, approaching the instrumental response function. Fitting requires a single decay constant of ~ 120 fs. Decay for 5 ML at this energy is significantly slower, displaying a strong asymmetry with pump-probe delay. Fitting requires at least two time constants: $\tau_1 \approx 200$ fs and $\tau_2 \approx 800$ fs, suggesting more complex decay dynamics.

At an intermediate energy [Fig. 3(b)], the faster decay for 1 ML is again apparent, but the data also indicate the emergence of an additional long-lived component for both films. Lifetimes determined from fits extending to long delays are on the order of $\tau_3 \approx 100-200$ ps; however, accurate determination is hampered by the maximum available pump-probe delay.

Cross correlations at the lowest energy [Fig. 3(c)] show the most marked divergence in behavior. The 5 ML curve rises monotonically to a maximum within <1 ps, followed by a very slow decay. In striking contrast, the 1 ML data exhibits an initial rise and then an ultrafast decrease until ~ 500 fs, followed by a subsequent increase requiring several picoseconds before reaching maximum. This indicates a delay between the loss of S_1 intensity above 0.4 eV, occurring on the order of hundreds of femtoseconds, and the later population increase at lower energies. As stated before, long time decay behavior is similar for both CuPc thicknesses.

To interpret these data, we consider processes involved in CuPc exciton decay. Cooling of the hot initial S_1 population through intraband vibrational relaxation will produce a downward shift of spectral weight with little loss of total intensity. This is consistent with the spectral downshift evident in the 5 ML data. Previous studies suggest time scales on the order of hundreds of femtoseconds for vibrational cooling in similar molecular systems; for example, a TR-2PPE study of ZnPc on TiO_2 reported a vibrational relaxation lifetime of 118 fs.[11]

Intersystem crossing (ISC) will transfer intensity from the excited singlet population to triplet levels. Triplet levels can be located based on phosphorescence ($T_1 \rightarrow S_0$) in CuPc films that has been measured at 1.12 eV.[20] CuPc triplet levels will thus appear close to 0 eV in Fig. 1. The long time constant, $\tau_3 \geq 100$ ps, observed in this energy region for both thicknesses is consistent with decay of a triplet exciton population. Furthermore, we find that the energy dependence of the amplitude fit values for this slow component yields a spectral peak centered at 0.06 ± 0.03 or 1.15 eV above the HOMO, consistent with identification of this component as the T_1 triplet. ISC time scales ranging from subpicosecond to picoseconds have been measured for metallophthalocyanines in solution and thin films.[21,22] CuPc, with its open-shell paramagnetic Cu^{2+} ion facilitating spin-orbit coupling, exhibits fast (picosecond) ISC, consistent with the absence of measurable fluorescence.[20]

At the interface, electron transfer results in loss of total intensity because the electron in C_{60} is not accessible in photoemission. For thick CuPc films, diffusion of the singlet exciton population from the surface to the interface could also decrease the 2PPE signal. A solution of the one-dimensional diffusion equation, $\partial/\partial t n(x,t) = [D\partial^2/\partial x^2] n(x,t)$, for the singlet population at the surface of a 5 nm CuPc film is plotted [Fig. 3(b)], assuming a very conservative upper bound value for the diffusion constant (10^{-2} cm^2 s^{-1}).[23] This simple simulation suggests that exciton diffusion is too slow to impact the loss of CuPc S_1 intensity observed with TR-2PPE for the 5 ML film.

Finally, at high excitation densities, decay via bimolecular exciton annihilation may occur. We estimate that the pump powers employed here result in exciton densities $<10^{18}$ cm^{-3}. This is well below the 10^{19} cm^{-3} threshold found for biexciton effects in previous work on H_2Pc films.[24] Significant biexciton effects are also not consistent with good fits to single exponential behavior and decay rates of hundreds of femtoseconds for cross correlation curves at high energy. However, without intensity-dependent data we cannot completely rule out some impact of biexciton decay at the very shortest time scales.

On the basis of these considerations, we suggest the following scenario to explain CuPc exciton dynamics as a function of CuPc thickness. The dominant processes are indicated in Fig. 1. This scenario is supported by investigations of photophysics for covalently bound porphryin- or phthalocyanine-fullerene dyads in solution.[25] For 5 ML, the initial small loss of total integrated intensity suggests dynamics dominated by spectral transfer, such as intraband cooling

and ISC. Intraband relaxation is also consistent with the downward spectral shift at high energy. Loss of S_1 population by ISC on picosecond time scales leads to a concurrent increase in population of lower T_1 levels. Subsequent triplet decay then occurs over at least hundreds of picoseconds. Loss due to exciton diffusion proceeds too slowly to impact the S_1 population. From a device point of view this implies that a significant fraction, if not a majority, of excitons reaching the C_{60} interfaces in a CuPc/C_{60} photovoltaic device arrive after conversion to triplets.

Proximity to the C_{60} substrate in the 1 ML structure has a dramatic impact. Ultrafast electron transfer to C_{60} results in the rapid decay of S_1 population on a time scale of $\sim$100 fs, outpacing ISC and intraband processes. The significant loss of total integrated intensity, by a factor >3 within the first 500 fs, is consistent with electron transfer to C_{60} levels. This also indicates that at the interface, charge transfer occurs for the hot-electron population before significant cooling can occur.

Charge transfer to C_{60} occurs into either "free" electron polaron levels or ICT levels. The location of C_{60} LUMO-based polaron levels from inverse photoemission data,[15] simulated in Fig. 2(b) as a dotted line, indicates that, for this interface, 1.65 eV pump-induced CuPc S_1 excitons do overlap C_{60} polaron levels, but without significant excess energy to assist charge separation. Alternatively, charge transfer can populate ICT states. These levels again are not evident in 2PPE due to attenuation by CuPc overlayers; nevertheless, their position can be estimated. The difference of $\sim$1.3 eV between the CuPc HOMO-C_{60} LUMO onsets provides an upper bound for the ICT energy. Coulomb interaction across the interface will reduce this energy. With a typical electron-hole binding energy of $\sim$0.3 eV, ICT states will most likely be located below CuPc singlet levels but above CuPc triplet states, making CuPc T_1 states the lowest manifold of excitations.

The implications of low-lying triplet levels on charge separation processes in organic photovoltaic systems have been topics of recent interest.[26,27] Enhanced triplet formation has been observed in F8BT:PFB polymer blends, where ISC is extremely slow in the pristine polymers, and attributed to increased ISC in the charge-transfer state where increased separation decreases the exchange energy. This opens a major route for recombination to polymer triplet levels at the interface. This process of triplet formation via ICT states provides a potential explanation for the delayed increase in the cross-correlation intensity at low energy for 1 ML. Electron transfer into C_{60} levels, most likely interfacial bound states, leads to the singlet dissociation on a time scale of $\sim$100 fs. We suggest that triplet formation in the ICT state provides a recombination route to intramolecular CuPc triplets, which appear after several picoseconds delay producing the intensity increase at low energy. We note that although this may provide a direct observation of the proposed recombination process, it may not have a significant influence in the CuPc/C_{60} system because ISC processes are already very fast, unlike the F8BT:PFB polymer blend case.

In summary, we have performed studies of dynamics at a well-characterized CuPc/C_{60} donor-acceptor interface using TR-2PPE. This work provides a detailed view of critical charge separation and recombination processes at this model interface and sets the stage for determining the impact of molecular orientation on interfacial carrier dynamics and device performance in organic photovoltaic structures. Electron transfer from CuPc S_1 levels to C_{60} is extremely efficient at the interface, but evidence also suggests that low-lying triplet levels lead to recombination back to CuPc triplets. Rapid ISC processes in CuPc suggest that diffusion and charge separation in the low-lying CuPc triplet manifold play an important role in photovoltaic efficiency for this system.

Support was provided by the National Science Foundation under MRSEC Program, Grant No. DMR-05-2047, the Surface Analytical Chemistry Program under Grant No. CHE0750203 and MRSEC shared equipment facilities. We also thank A. Hamins-Puertolas for initial data analysis and D. B. Dougherty for experimental assistance.

[1] B. A. Gregg, J. Phys. Chem. B **107**, 4688 (2003).
[2] Y. Yi, V. Coropceanu, and J.-L. Bredas, J. Am. Chem. Soc. **131**, 15777 (2009).
[3] C. J. Brabec *et al.*, Chem. Phys. Lett. **340**, 232 (2001).
[4] I.-W. Hwang, D. Moses, and A. J. Heeger, J. Phys. Chem. C **112**, 4350 (2008).
[5] O. Esenturk *et al.*, J. Phys. Chem. C **113**, 18842 (2009).
[6] A. C. Morteani, P. Sreearunothai, L. M. Herz, R. H. Friend, and C. Silva, Phys. Rev. Lett. **92**, 247402 (2004).
[7] D. Veldman, S. C. J. Meskers, and R. A. J. Janssen, Adv. Funct. Mater. **19**, 1939 (2009).
[8] C. D. Lindstrom and X. Y. Zhu, Chem. Rev. **106**, 4281 (2006).
[9] M. Muntwiler, Q. Yang, W. A. Tisdale, and X.-Y. Zhu, Phys. Rev. Lett. **101**, 196403 (2008).
[10] L. Gundlach, R. Ernstorfer, and F. Willig, Prog. Surf. Sci. **82**, 355 (2007).
[11] D. Ino *et al.*, J. Phys. Chem. B **109**, 18018 (2005).
[12] J. Xue *et al.*, J. Appl. Phys. **98**, 124903 (2005).
[13] H. Huang *et al.*, Appl. Phys. Lett. **94**, 163304 (2009).
[14] W. Jin, Ph.D. thesis, University of Maryland, 2010.
[15] R. Hesper, L. H. Tjeng, and G. A. Sawatzky, Europhys. Lett. **40**, 177 (1997).
[16] O. V. Molodtsova and M. Knupfer, J. Appl. Phys. **99**, 053704 (2006).
[17] E. A. Lucia and F. D. Verderame, J. Chem. Phys. **48**, 2674 (1968).
[18] A. Skumanich, Chem. Phys. Lett. **182**, 486 (1991).
[19] G. Dutton and X. Y. Zhu, J. Phys. Chem. B **108**, 7788 (2004).
[20] K. Yoshino *et al.*, J. Phys. Soc. Jpn. **34**, 441 (1973).
[21] R. R. Millard and B. I. Greene, J. Phys. Chem. **89**, 2976 (1985).
[22] G. Ma *et al.*, Solid State Commun. **118**, 633 (2001).
[23] R. R. Lunt *et al.*, J. Appl. Phys. **105**, 053711 (2009).
[24] B. I. Greene and R. R. Millard, Phys. Rev. Lett. **55**, 1331 (1985).
[25] M. Niemi *et al.*, J. Phys. Chem. A **112**, 6884 (2008).
[26] T. A. Ford, I. Avilov, D. Beljonne, and N. C. Greenham, Phys. Rev. B **71**, 125212 (2005).
[27] S. Westenhoff *et al.*, J. Am. Chem. Soc. **130**, 13653 (2008).